J Prosthodont Res. 2024; 68(3): 474–481

OPEN ACCESS

Journal of Prosthodontic Research

Original article

In silico nonlinear dynamic finite-element analysis for biaxial flexural strength testing of CAD/CAM materials

Hefei Li [a], Satoshi Yamaguchi [a,*], Chunwoo Lee [a], Ernesto B. Benalcázar-Jalkh [b], Estevam A. Bonfante [b], Satoshi Imazato [a]

[a] Department of Dental Biomaterials, Osaka University Graduate School of Dentistry, Suita, Japan, [b] Department of Prosthodontics and Periodontology, University of São Paulo, Bauru School of Dentistry, Bauru, Brazil

Abstract

Purpose: The aim of this study was to establish and assess the validity of *in silico* models of biaxial flexural strength (BFS) tests to reflect *in vitro* physical properties obtained from two commercially available computer-aided design/computer-aided manufacturing (CAD/CAM) ceramic blocks and one CAD/CAM resin composite block.

Methods: *In vitro* three-point bending and BFS tests were conducted for three CAD/CAM materials (n = 10): Katana Zirconia ST10 (raw material: super-translucent multilayered zirconia, ST10; Kuraray Noritake Dental, Niigata, Japan), Katana Zirconia HT10 (raw material: highly translucent multilayered zirconia, HT10; Kuraray Noritake Dental), and Katana Avencia N (AN; Kuraray Noritake Dental). Densities, flexural moduli, and fracture strains were obtained from the *in vitro* three-point bending test and used as an input for an *in silico* nonlinear finite element analysis. The maximum principal stress (MPS) distribution was obtained from an *in silico* BFS analysis.

Results: The elastic moduli of AN, HT10, and ST10 were 6.513, 40.039, and 32.600 GPa, respectively. The *in silico* fracture pattern of ST10 observed after the *in silico* evaluation was similar to the fracture pattern observed after the *in vitro* testing. The MPS was registered in the center of the tensile surface for all three specimens. The projections of the supporting balls were in the form of a triple asymmetry.

Conclusions: The *in silico* approach established in this study provided an acceptable reflection of *in vitro* physical properties, and will be useful to assess biaxial flexural properties of CAD/CAM materials without wastage of materials.

Keywords: CAD-CAM, Y-TZP Ceramic, Composite Resins, Finite-Element Analysis, Flexural Strength

Received 18 January 2023, Accepted 13 October 2023, Available online 3 January 2024

1. Introduction

Advances in dental computer-aided design/computer-aided manufacturing (CAD/CAM) processes have led to the expanding use of machinable ceramic blocks[1]. Recently, monolithic multilayered zirconia ceramics have been developed and have become preferable materials to produce dental restorations by clinicians due to their counterbalanced mechanical and aesthetic properties[2]. They have a better semblance to the natural tooth structure consisting of different layers with varying degrees of translucency and color intensity[3,4]. The mechanical properties of certain types of commercially available multilayered zirconia blocks have been evaluated using *in vitro* test setups[5–7].

Flexural strength is generally considered a meaningful and reliable parameter to evaluate mechanical properties of restorative or prosthetic materials. It is often determined by an *in vitro* three-point/four-point bending test[8–10]. Although the three-point bending test is the most commonly used method, there is sensitivity to flaws along specimen edges or surface defects. This may result in failure of the test beam at a location that is not directly beneath the applied load, thereby violating the testing apparatus and possibly yielding inaccurate outcomes[11,12]. Another method to determine the flexural strength of ceramic materials is the biaxial flexural strength (BFS)

WHAT IS ALREADY KNOWN ABOUT THE TOPIC?

» *In vitro tests for measuring the flexural strength of CAD/CAM zirconia ceramics typically provide inaccurate results and can result in material wastage. Finite element analysis (FEA) allows the assessment of stress distribution and evaluation of various mechanical performance parameters. An FEA-based approach that can accurately assess in vitro biaxial flexural properties has not yet been reported.*

WHAT THIS STUDY ADDS?

» *Our study proposed an FEA approach that accurately mirrors in vitro load–displacement curves, biaxial flexural strength, and fracture patterns of the studied materials. Fracture behavior varied between CAD/CAM zirconia and resin composite blocks owing to stress triaxiality thresholds, highlighting the need for clinicians to consider various stress states concentrated in restorations.*

DOI: https://doi.org/10.2186/jpr.JPR_D_23_00008

***Corresponding author:** Satoshi Yamaguchi, Department of Dental Biomaterials, Osaka University Graduate School of Dentistry, 1-8 Yamadaoka, Suita, Osaka 565-0871, Japan.

E-mail address: yamaguchi.satoshi.dent@osaka-u.ac.jp

Table 1. Composition of CAD/CAM resin composites used in this study

	Code	Manufacturer	Composition	Content (wt%)
Katana Avencia N	AN	Kuraray Noritake Dental	Mixed filler with colloidal silica and aluminum oxide Cured resins consisting of methacrylate monomer (Copolymer of Urethane dimethacrylate and other methacrylate monomers)	62%
Katana™ Zirconia ST10 (raw material of STML)	ST10		ZrO_2+HfO_2	88%-93%
			Y_2O_3	7%-10%
			Others	0%-2%
Katana™ Zirconia HT10 (raw material of HTML)	HT10		ZrO_2+HfO_2	90%-95%
			Y_2O_3	5%-8%
			Others	0%-2%

test. Under biaxial flexural conditions, the maximum tensile stress occurs in the bottom of the central loading area within the specimen, which prevents the premature failure from edge flaws[11]. As dental restorations are subjected to multiaxial mastication forces with a considerable amount of flexural stresses in the oral cavity, BFS tests would be advantageous to simulate the relative properties of restorative and prosthetic materials[1,13]. Different loading configurations have been identified, such as piston-on-three-ball (P3B)[14,15], piston-on-ring[16], ball-on ring (BOR)[17], and ring-on-ring[18]. Only the P3B test has been adopted by International Organization for Standardization (ISO) 6872: 2015 among the above methods, in which a thin disc is supported by three balls and loaded by a piston.

However, for both *in vitro* uniaxial and BFS tests, inaccuracies may occur during specimen–fixture articulation, positioning, and parallelism[19]. The preparation of a minimized specimen for the BFS test using such brittle materials can be time-consuming and material-wasting. Additionally, different flexural strength values of the same product have been reported by different researchers and manufacturers as the behavior of ceramics can be susceptible to different specimen processing and testing conditions including the sintering and surface polishing methods, thickness and geometry of the specimen, and type of loading piston[8,19–24].

Although finite-element analysis (FEA) is digitally available for these parameters, as well as those of the preparations, it is more amenable to a stress analysis and failure prediction[25]. FEA has been well established as a method for assessment of the stress distribution in dental materials, with numerous advantages including specimen standardization, low cost, and capability to detect a fracture initiation point from stress concentration regions[26,27]. Compared to *in vitro* studies, FEA allows evaluation of the stress distribution as a subject of analysis for the assessment of diverse physical parameters related to mechanical performance[28]. Therefore, a standard *in silico* method, which reduces the repeating times of an *in vitro* experiment, while reflecting *in vitro* mechanical properties, should be considered.

Nonlinear dynamic FEA can represent fracture propagation corresponding to the fracture criteria of materials[29]. The fracture criterion is one of the important factors to obtain accurate fracture loads reflecting the *in vitro* results. In one study, the maximum principal strain has been reported as the most appropriate fracture criterion for evaluation of the flexural strength of resin composites[30]. In our previous study, an *in silico* three-point bending and notchless triangular prism model was developed and reflected *in vitro* physical properties of CAD/CAM resin composite blocks (RCBs) using the maximum principal strain as a fracture criterion[27]. Thus, we conceive an approach to combine the nonlinear dynamic FEA and fracture criterion to develop *in silico* models of BFS tests to reflect the *in vitro* results for both materials.

To the best of our knowledge, *in silico* approach that can reflect the biaxial flexural properties (load–displacement curves, BFS, fracture patterns) without conducting the BFS test has not been reported. Based on the *in silico* process that we have established in previous studies[27,30], the aim of this study was to further assess the validity of *in silico* models of BFS tests to reflect *in vitro* physical properties obtained from two commercially available CAD/CAM ceramic blocks and one CAD/CAM resin composite block. The null hypothesis was that the proposed *in silico* approach could not reflect the *in vitro* biaxial flexural properties obtained from the tested materials.

2. Materials and Methods

2.1. CAD/CAM blocks

Three commercially available CAD/CAM blocks were used: Katana Zirconia ST10 (raw material: super-translucent multilayered (STML) zirconia, ST10; Kuraray Noritake Dental, Niigata, Japan), Katana Zirconia HT10 (raw material: highly translucent multilayered (HTML) zirconia, HT10; Kuraray Noritake Dental), and Katana Avencia N (AN; Kuraray Noritake Dental). Details of the material composition of each block are summarized in **Table 1**.

2.2. In vitro three-point bending tests

In vitro three-point bending tests were conducted for the three CAD/CAM materials (n = 10). Regarding the CAD/CAM RCB, 1.2 × 4 × 14 mm^3 rectangular bar specimens were prepared using a diamond-coated low-speed precision sectioning blade (ISOMET1000, Buehler, Illinois, USA) and polished with #1000 and #2000 SiC papers. The specimens were immersed in distilled water at 37 °C for 24 h. Regarding the CAD/CAM ceramic blocks, 60 × 50.5 × 21 mm^3 rectangular specimens were prefabricated using a milling machine (DWX-52DC, Roland DG, Shizuoka, Japan) and fired at 1500 °C for 2 h using a furnace (Noritake Katana F-1 N, Kuraray Noritake Dental) according to the manufacturer's recommendations. By trimming the specimens using a diamond saw, rectangular bar specimens (1.5 × 4 × 18 mm^3) were obtained. *In vitro* three-point bending tests were conducted using a universal testing machine (EZ-SX, Shimadzu, Kyoto, Japan) with a crosshead speed of 1 mm/min.

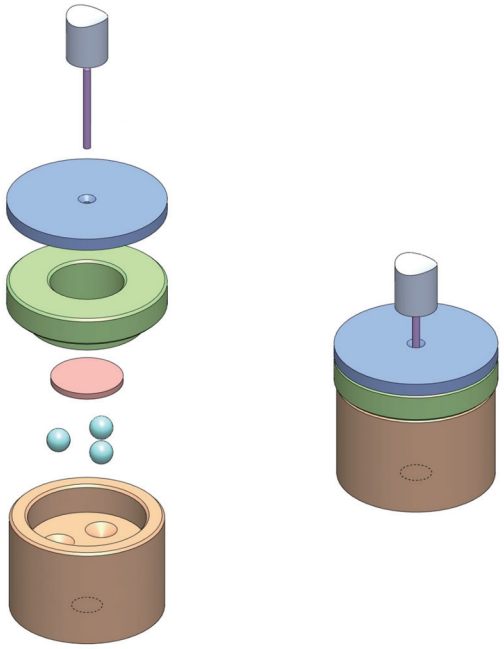

Fig. 1. CAD models of the *in vitro* biaxial flexural strength test for fabrication of custom-made jigs

2.3. Preparation of specimens for the biaxial flexural test

The *in vitro* BFS test was conducted for three CAD/CAM materials (n = 10). Regarding the CAD/CAM resin composite block, φ14 × 1.2 mm^2 cylindrical disk specimens were fabricated using a machining center (VM5, OKK, Hyogo, Japan) and grinding machine (MHT, Mitsui High-tec, Fukuoka, Japan). These specimens were polished with #1000 and #2000 SiC papers. Regarding the CAD/CAM ceramic blocks, disk-shaped specimens (φ17 × 1.5 mm^2) were fabricated using a milling machine (DWX-52DC, Roland DG) and fired at 1500 °C for 2 h using a furnace (Noritake Katana F-1 N, Kuraray Noritake Dental) to obtain specimens with final dimensions of φ14 × 1.2 mm^2.

2.4. In vitro BFS test

According to the ISO 6872: 2014 standard, a custom-made P3B biaxial fixture was prepared. The specimens for each material were supported by three stainless-steel ball bearings with a diameter of 4.5 ± 0.1 mm positioned 120° apart on a support circle with a diameter of 11 mm. The load was applied with a flat piston with a diameter of 1.4 mm at the center of the specimen using a universal testing machine (AG-X plus, Shimadzu) with a constant crosshead speed of 1 mm/min. A schematic of the experimental setup is presented in **Figure 1**. The BFS ($\sigma_{biaxial}$) was determined by

$$\sigma_{biaxial} = \frac{-0.2387P(X-Y)}{b^2},$$

where P is the total load causing fracture [N], b is the thickness of the specimen [mm], and X and Y are determined by

$$X = (1+\nu)\ln\left(\frac{r_2}{r_3}\right)^2 + \left[\frac{(1-\nu)}{2}\right]\left(\frac{r_2}{r_3}\right)^2,$$

$$Y = (1+\nu)\left[1+\ln\left(\frac{r_1}{r_3}\right)^2\right] + (1-\nu)\left(\frac{r_1}{r_3}\right)^2,$$

where ν (0.38) is the Poisson's ratio, r_1 (5.5 mm) is the radius of the support circle, r_2 (0.7 mm) is the radius of the loaded area, and r_3 (7 mm) is the radius of the specimen.

2.5. In silico three-point bending tests

In silico three-point bending analyses were conducted for the three materials using the nonlinear dynamic FEA (LS-DYNA, ANSYS, Pennsylvania, USA). The FEA models were designed using a pre- and post-processor (LS-PrePost, ANSYS) according to the specimen dimensions. Two important parameters were considered for the FEA file, the density and elastic modulus. For each specimen, the volume was measured by microcomputed tomography (micro-CT; R_mCT2, Rigaku, Tokyo, Japan) at a resolution of 0.05 × 0.05 × 0.05 mm^3 and voltage of 90 kVp. The density was calculated by dividing the weight measured by an analytical balance (AP124X, Shimadzu) by the volume. To assess the elastic modulus, the load–displacement curve obtained by the *in vitro* three-point bending test was converted into a stress–strain curve. The flexural modulus was obtained by the initial slope of the stress–strain curve. The fracture strain was recorded at the end of the curve. The flexural modulus and elastic modulus are not equal. However, the flexural modulus was used as an initial trail value for the three-point bending FEA file. After the first analysis, the load–displacement curves exhibited some differences from the *in vitro* load–displacement curve. We then changed the flexural modulus value according to the difference and calculated again. This process was repeated until the *in silico* and *in vitro* curves were converged within an error of 10%. The final value was then determined as the elastic modulus. The Poisson's ratio of each material was set to 0.38 according to that of dental composites[31].

2.6. Failure criteria selection

For AN, MAT_ADD_EROSION was used to control the element erosion. The maximum principal stress (MPS) was obtained from the three-point bending *k* file, which showed the last converged curve, and was used as an input failure criterion for the *in silico* biaxial flexural test. Regarding HT10 and ST10, the effective plastic strain (EPS) was obtained from the three-point bending *k* file, which showed the last converged curve, and was used as an input failure criterion for the *in silico* BFS test. MAT_ADD_DAMGE_GISSMO was used to control the element erosion. The stress triaxiality factor was set to 0.333 for the three-point bending simulation and 0.667 for the BFS test simulation. The corresponding erosion keywords and failure criteria are shown in **Table 2**. The theoretical background of the GISMMO model used in MAT_ADD_DAMAGE_GISSMO is summarized in **Supplementary information**.

Table 2. Erosion keywords and failure criterion used in LS-DYNA

	Erosion keyword	Failure criteria
AN	MAT_ADD_EROSION	Maximum principal stress
HT10	MAT_ADD_DAMAGE_GISSMO	Effective plastic strain
ST10	MAT_ADD_DAMAGE_GISSMO	Effective plastic strain

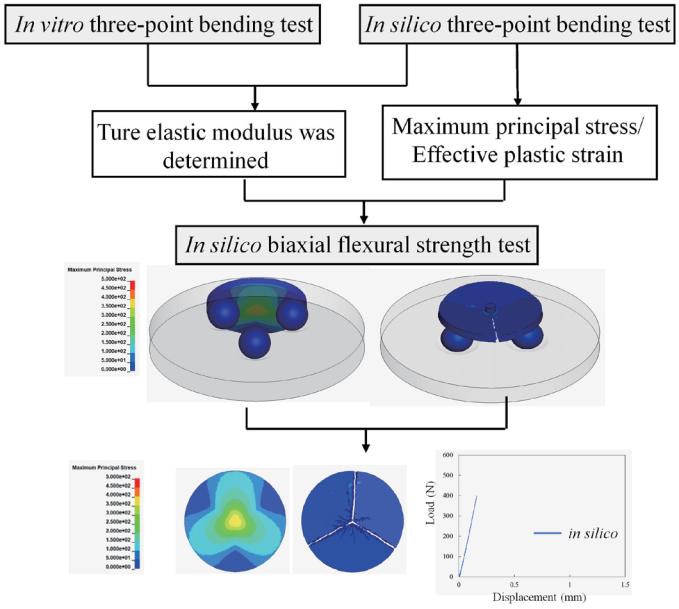

Fig. 2. Schematic for an *in silico* biaxial flexural strength analysis

2.7. In silico BFS analysis

The CAD models for the *in silico* BFS analysis were designed according to the same parameters as for the *in vitro* jigs. Using the elastic moduli and EPS obtained from the *in vitro* three-point bending test, along with densities, a nonlinear dynamic FEA was conducted. Load–displacement curves, BFS for each analysis, and fracture patterns were obtained and compared to *in vitro* results. The MPS distribution was obtained at each calculation point for the three materials. A schematic of the whole process is shown in **Figure 2**.

2.8. Fracture pattern analysis

The fracture pattern of the disk specimens for AN, HT10, and ST10 after *in vitro* BFS tests was observed by optical microscopy (SMZ-745T, Nikon, Tokyo, Japan) at a magnification of 0.67×. Both *in vitro* and *in silico* fracture patterns were compared.

2.9. Statistical analysis

Loads and displacement at each time point obtained from the *in vitro* BFS tests were compared statistically to the value determined by an *in silico* analysis using Spearman's correlation tests (IBM SPSS Statistics 25, IBM, New York, USA). Regarding the HT10 and ST10 blocks, *in silico* curves were also fitted by a linear dotted line. The correlation analysis was conducted between this fitted linear curve (translated along the *X* axis to the origin) and *in vitro* curve. *P* values below 0.05 were considered statistically significant for all tests.

Table 3. Physical properties of three materials obtained by *in vitro* three-point bending tests, micro-CT analysis, and weight measurement

	Flexural modulus (GPa)	Density (g/cm^3)	Fracture strain (ε)
AN	6.913±0.207	1.66±0.00783	0.0491±0.00319
HT10	39.661±0.700	6.01±0.01202	0.0330±0.00078
ST10	33.081±2.009	5.96±0.13462	0.0228±0.00286

3. Results

3.1. Elastic modulus obtained from the in silico three-point bending analysis

The flexural moduli, densities, and fracture strains of AN, HT10, and ST10 are summarized in **Table 3**. *In vitro/in silico* load–displacement curves after the three-pointing tests/analysis are shown in **Figure 3**. The *in vitro* curves were obtained by averaging all loads and displacement at each time point. Both *in vitro* and *in silico* load–displacement curves were significantly correlated (AN: R_{Load} = 1.000, HT10: R_{Load} = 0.997, ST10: R_{Load} = 0.997; AN: $R_{Displacement}$ = 0.999, HT10: $R_{Displacement}$ = 0.997, ST10: $R_{Displacement}$ = 0.997, $P < 0.05$). The elastic moduli of AN, HT10, and ST10 were 6.513, 40.039, and 32.600 GPa, respectively.

3.2. Flexural strength after the in vitro/in silico biaxial flexural test/analysis

The mean BFSs obtained by the *in vitro/in silico* biaxial test/analysis for the three materials are listed in **Table 4**. *In vitro/in silico* load–displacement curves after the BFS tests/analysis are shown in **Figure 4**. The *in vitro* curve was obtained by averaging all loads and displacement at each time point. Both *in vitro* and *in silico* load–displacement curves were significantly correlated (AN: R_{Load} = 1.000, HT10: R_{Load} = 1.000, ST10: R_{Load} = 1.000; AN: $R_{Displacement}$ = 1.000, HT10: $R_{Displacement}$ = 1.000, ST10: $R_{Displacement}$ = 1.000, $P < 0.05$).

3.3. MPS distribution in the disk specimens

Figure 5 shows the MPS distribution during deformation and after fracture for AN, HT10, and ST10. The MPS was registered in the center of the tensile surface for all three specimens with a gradual decrease to its borders. The MPS distribution and projections of the supporting balls were in the form of a triple asymmetry. A fracture was observed after the MPS exceeded the fracture stress of each material on the tensile side.

3.4. Fracture pattern analysis

The fracture patterns of the disk specimens for AN, HT10, and ST10 after *in vitro* and *in silico* BFS tests/analysis are presented in **Figures 6a and b**. The fracture pattern of ST10 observed after the *in silico* evaluation was similar to the fracture pattern observed after the *in vitro* testing.

4. Discussion

Previously, we have established an *in silico* three-point bending and notchless triangular prism model and reflected *in vitro* physical properties of CAD/CAM resin composites[27]. To further elucidate the effectiveness of this *in silico* approach, in this study, we developed a

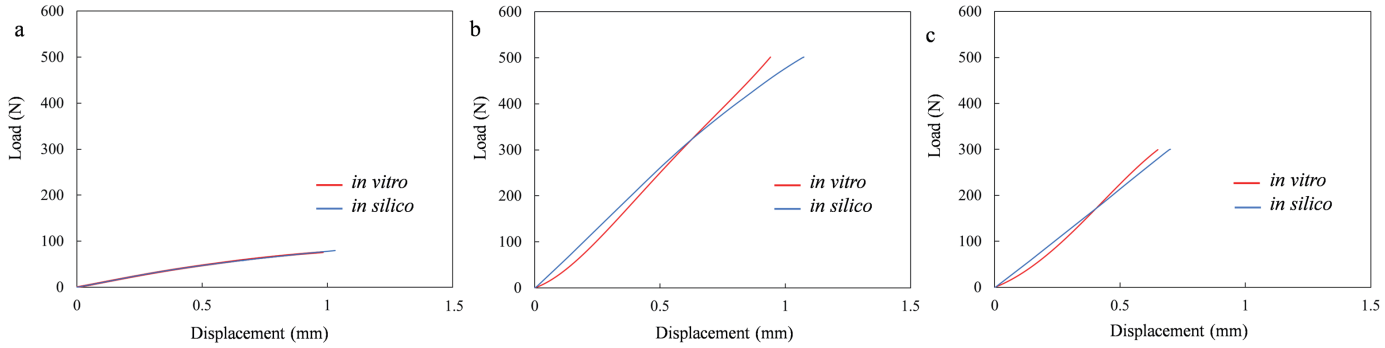

Fig. 3. Load–displacement curve obtained from *in vitro/in silico* three-point bending tests. The *in vitro* curve was obtained by averaging all curves. a: AN, b: HT10, c: ST10.

Table 4. Mean biaxial flexural strength values obtained from *in vitro/in silico* biaxial test/analysis

	Biaxial flexural strength (MPa)	
	in vitro	*in silico*
AN	274.235±29.630	275.362
HT10	620.560±63.376	605.055
ST10	489.338±22.303	502.566

biaxial flexural test model that could be used to predict BFS to reflect *in vitro* physical properties obtained from two commercially available CAD/CAM zirconia blocks and one RCB. The null hypothesis was rejected as the *in vitro/in silico* load–displacement curves after the BFS tests/analysis were significantly correlated.

Under the conditions of our study, for AN, the same *in silico* approach described in the previous study[27] was applied and reflected the *in vitro* load–displacement curve. However, for both zirconia blocks, different erosion method and failure criteria were applied, as described in the Materials and Methods section, and reflected the *in vitro* properties. These first reported keyword settings could provide meaningful references for future FEA for dental zirconia. Furthermore, the *in silico* approach employed in this study, which utilizes the nonlinear dynamic FEA, demonstrated that the fracture behavior of CAD/CAM zirconia blocks differs from those of CAD/CAM resin composites because of a varying threshold depending on the stress triaxiality. This finding suggests that clinicians should be mindful to the various stress states that concentrate in dental restorative materials.

The three-point bending tests indicated that the elastic modulus of AN was considerably lower than those of HT10 and ST10. The elastic modulus represents the stiffness of a material within the elastic range when tensile or compressive forces are applied[32]. Ceramics usually have higher moduli than polymers and composites, and therefore are stiffer and more brittle[33]. For yttria-stabilized zirconia (YSZ) blocks, the elastic modulus of HT10 was barely higher than that of ST10. **Table 1** shows that the yttria exhibited differences among these two materials. However, the yttria content has a limited effect on the elastic modulus of dental zirconia[34].

In a previous study, we used an *in silico* three-point bending analysis to reflect the *in vitro* testing of CAD/CAM RCBs[27]. In this study, the proposed models for *in silico* analyses also reflected the *in vitro* testing results of one CAD/CAM RCB and two zirconia blocks. These results suggested that, using this *in silico* approach, the three-point bending test would be the only *in vitro* experiment required to obtain the flexural modulus. Thereafter, the elastic modulus could be calculated by the *in silico* three-point bending analysis, and the obtained elastic modulus could be used as an input parameter for other mechanical tests, such as BFS or four-point bending tests. The established approach has been applied to CAD/CAM resin composite crowns, by subjecting them to a compression test[35], and will be useful for prediction of the crack initiation point of marginal/incisal chippings for zirconia crowns[36] or design of the appropriate crown shape to prevent an unexpected failure.

The BFS test was originally developed for brittle ceramic or glassy materials. The equations for BFS calculation were proposed by Kirstein and Woolley[37]. The applications of BFS testing have expanded as an alternative protocol to overcome the shortcomings of the traditional uniaxial three-point bending test for measurements of flexural properties of dental materials[34,38] such as CAD/CAM RCBs and ceramic blocks. Notably, for both zirconia blocks, the load–displacement curves exhibited a nonlinear part in the beginning. This phenomenon could be attributed to the unstable contact at the initial stage. Owing to the hardness of zirconia, it was difficult to slightly deform and fully contact with the supporting balls, inducing a period of an unstable curve, which could not reflect the intrinsic material property. Compared to HT10 and ST10, AN tended to be softer. Therefore, the resin composite specimen more easily exhibits a slight deformation and starts the normal contacting process, and thus the slope did not show notable change. This nonlinear part could also originate from the difference between *in vitro* and *in silico* specifications of the specimens and fixations. *In vitro,* the sizes of the three stainless steel supporting balls were not exactly equal. There were slight differences among them, within the standard deviations (±0.1 mm). Therefore, the contact surface between the specimen and supporting jigs was not completely flat, which resulted in an unstable contact at the initial stage of the BFS test. However, in the *in silico* scenario, the specifications of both specimen and supporting jigs are exactly the same. Without space between the specimen and supporting balls, the contact surface was ideal. Considering this setup, the contact between the supporting fixture and tested specimens was stable from the initial stage. In other words, the degree of freedom for the *in vitro* test was larger than in the *in silico* simulation.

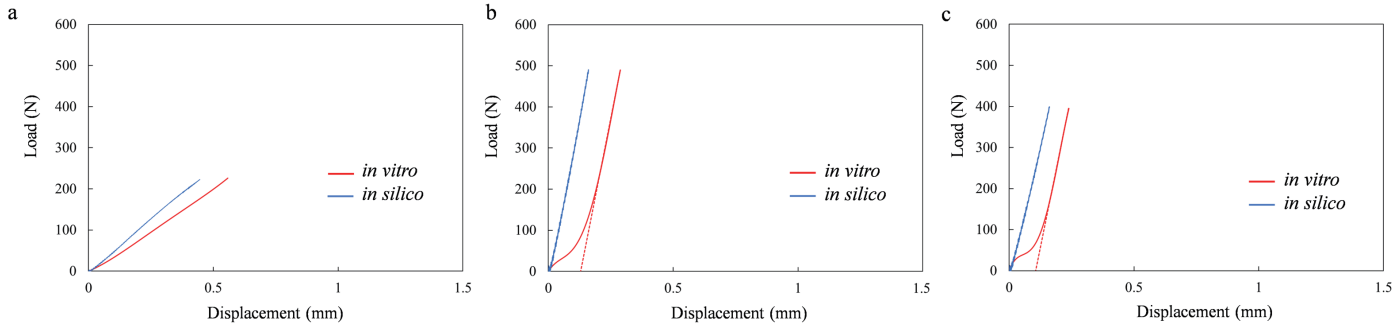

Fig. 4. Load–displacement curve obtained from *in vitro*/*in silico* biaxial flexural strength tests. The *in vitro* curve was obtained by averaging all curves. a: AN, b: HT10, c: ST10.

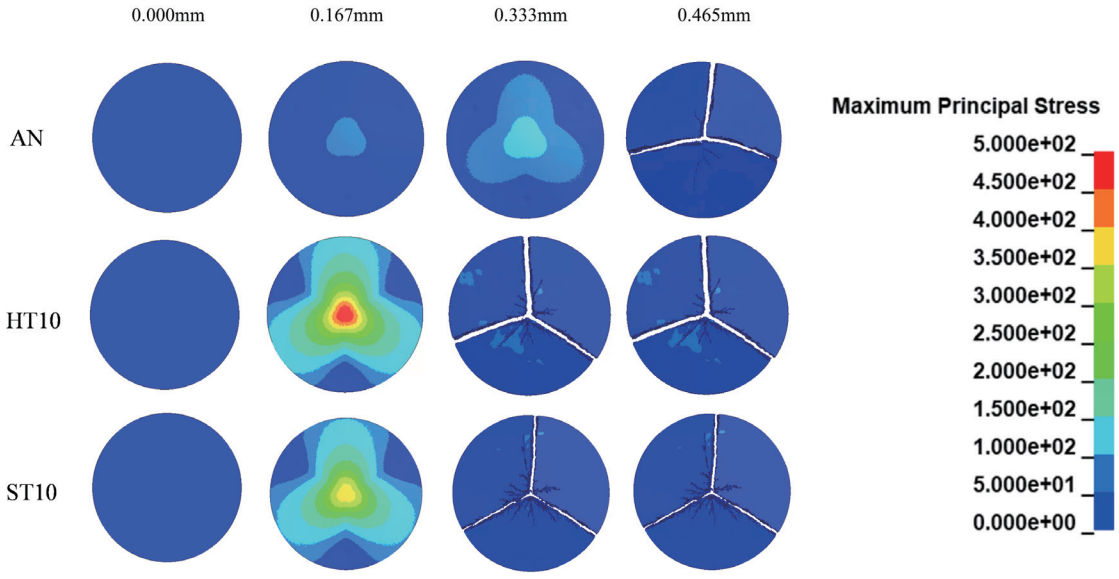

Fig. 5. Maximum principal stress distribution at each calculation point. 0.000, 0.167, 0.333, and 0.465 mm from left to right.

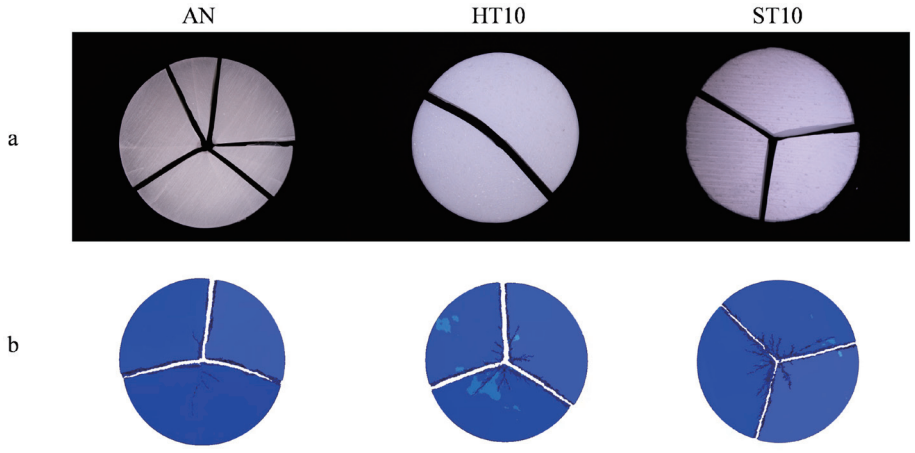

Fig. 6. Fracture patterns of three materials after *in vitro*/*in silico* biaxial flexural strength tests. a: *in vitro*, b: *in silico*.

The BFSs of HT10 and ST10 were higher than that of AN. Zirconia has no intervening etchable glassy matrix. All crystals are densely packed into regular arrays, and then sintered[39,40]. The dense crystal lattice reduces crack propagation resulting in stronger mechanical properties[41]. For YSZ, the BFS of HT10 was higher than that of ST10. According to the material compositions in **Table 1**, the yttria content of ST10 was 7–10 wt%, higher than that of HT10 (5–8 wt%). In case of not considering other effective factors, a higher yttria content corresponds to a better translucency at the expense of lower strength and toughness[3]. The BFS for STML is consistent with those of Pereira *et al.* (487.6–528.5 MPa)[42] and Kongkiatkamon *et al.* (466.41 ± 22.898 MPa)[43], but lower than that of another study, where plate-shaped specimens were used, instead of disk-shaped specimens, which was not a requirement from the ISO standard 6872[6]. The BFSs for HT10 and AN have not been reported in the published studies.

The strength is not an inherent property of a material, and therefore the recorded value by the *in vitro* test is a function of the geometry and preparation of the specimen, as well as the testing method[12]. However, our developed approach could reflect the inherent strength and elastic properties of the materials, which could not be affected by the error caused by fixations and specimen preparation process.

In terms of fracture pattern, the *in silico* simulation demonstrated a fracture pattern for the ST10 block that closely matched the observed *in vitro* fracture patterns, which further suggested the effectiveness of our proposed method. There has been a positive correlation between fractured pieces and strength values in a BOR-configuration BFS test for RCBs[13]. However, both of our *in vitro*/*in silico* results for zirconia with the P3B configuration did not reveal the same trend. HT10 had a higher BFS but less fragments compared to ST10. This result could be explained by the different materials and configurations used. As a discrete population of internal flaws exists in the specimens' structure in zirconia[6] or voids, various filler shapes, and distribution in CAD/CAM RCBs, the fracture pattern could be affected, leading to different fracture patterns compared to the results from FEA, where the fracture pattern was obtained from a perfectly homogeneous zirconia or CAD/CAM RCBs. Therefore, the *in vitro* fracture fragments of AN and HT10 were not the same, regarding the results of *in silico* simulations.

The MPS distribution concentrated in the middle at the bottom of the specimen with a gradual decrease toward the specimen borders, as shown in **Figure 5**. This distribution was similar to that of the FEA simulation conducted by Čokić *et al.* even though their mesh size was 0.2 mm[6]. The mesh size for the developed models was 0.1 mm. It was still relatively large to represent the crack initiation and crack propagation compared to the nano/microscale. Therefore, the combination of the multiscale analysis and FEA[27] should be considered to achieve a direct observation of the fracture behavior of composites with nanofillers at the nano/microscale in the future. One of the limitations of this study is that the elastic modulus of multilayer zirconia ceramics may vary in different layers. Future studies considering the different elastic modulus of each layer in anatomic models are required to investigate the fracture origin and crack propagation of zirconia crowns. Additionally, in the future, this approach, involving the *in vitro* mechanical testing of materials and *in silico* FEA simulation, should be further validated by other testing centers.

5. Conclusions

The *in silico* approach established in this study produced results that were similar and correlated with the *in vitro* biaxial flexural properties of the tested CAD/CAM RCBs and ceramic blocks. The established approach will be useful to assess biaxial flexural properties of CAD/CAM RCBs and ceramics without wastage of materials.

Acknowledgements

This study was supported by São Paulo Reuter Foundation (FAPESP), grants #2021/06730-7 and #2022/07157-1. We thank Kuraray Noritake Dental for the donation of some of the materials.

Conflict of interest

The authors declare no conflict of interest.

References

[1] Sen N, Us YO. Mechanical and optical properties of monolithic CAD-CAM restorative materials. J Prosthet Dent. 2018;119:593–9. https://doi.org/10.1016/j.prosdent.2017.06.012, PMID:28781072

[2] Elsaka SE. Optical and mechanical properties of newly developed monolithic multilayer zirconia. J Prosthodont. 2019;28:e279–84. https://doi.org/10.1111/jopr.12730, PMID:29239067

[3] Kolakarnprasert N, Kaizer MR, Kim DK, Zhang Y. New multi-layered zirconias: Composition, microstructure and translucency. Dent Mater. 2019;35:797–806. https://doi.org/10.1016/j.dental.2019.02.017, PMID:30853208

[4] Zhang Y, Lawn BR. Novel zirconia materials in dentistry. J Dent Res. 2018;97:140–7. https://doi.org/10.1177/0022034517737483, PMID:29035694

[5] Bruhnke M, Awwad Y, Müller WD, Beuer F, Schmidt F. Mechanical properties of new generations of monolithic, multi-layered zirconia. Materials (Basel). 2022;16:276. https://doi.org/10.3390/ma16010276, PMID:36614613

[6] Čokić SM, Cóndor M, Vleugels J, Meerbeek BV, Oosterwyck HV, Inokoshi M, *et al.* Mechanical properties–translucency–microstructure relationships in commercial monolayer and multilayer monolithic zirconia ceramics. Dent Mater. 2022;38:797–810. https://doi.org/10.1016/j.dental.2022.04.011, PMID:35450705

[7] Kaizer MR, Kolakarnprasert N, Rodrigues C, Chai H, Zhang Y. Probing the interfacial strength of novel multi-layer zirconias. Dent Mater. 2020;36:60–7. https://doi.org/10.1016/j.dental.2019.10.008, PMID:31727444

[8] Xu Y, Han J, Lin H, An L. Comparative study of flexural strength test methods on CAD/CAM Y-TZP dental ceramics. Regen Biomater. 2015;2:239–44. https://doi.org/10.1093/rb/rbv020, PMID:26816646

[9] Furtado de Mendonca A, Shahmoradi M, Gouvêa CVD, De Souza GM, Ellakwa A. Microstructural and mechanical characterization of CAD/CAM materials for monolithic dental restorations. J Prosthodont. 2019;28:e587–94. https://doi.org/10.1111/jopr.12964, PMID:30121945

[10] Ferracane JL, Hilton TJ, Stansbury JW, Watts DC, Silikas N, Ilie N, *et al.* Academy of Dental Materials guidance—Resin composites: part II—Technique sensitivity (handling, polymerization, dimensional changes). Dent Mater. 2017;33:1171–91. https://doi.org/10.1016/j.dental.2017.08.188, PMID:28917571

[11] Lin WS, Ercoli C, Feng C, Morton D. The effect of core material, veneering porcelain, and fabrication technique on the biaxial flexural strength and weibull analysis of selected dental ceramics. J Prosthodont. 2012;21:353–62. https://doi.org/10.1111/j.1532-849X.2012.00845.x, PMID:22462639

[12] Ilie N, Hilton TJ, Heintze SD, Hickel R, Watts DC, Silikas N, *et al.* Academy of Dental Materials guidance-Resin composites: part I-Mechanical properties. Dent Mater. 2017;33:880–94. https://doi.org/10.1016/j.dental.2017.04.013, PMID:28577893

[13] Choi BJ, Yoon S, Im YW, Lee JH, Jung HJ, Lee HH. Uniaxial/biaxial flexure strengths and elastic properties of resin-composite block materials for CAD/CAM. Dent Mater. 2019;35:389–401. https://doi.org/10.1016/j.dental.2018.11.032, PMID:30527587

[14] Ozturk C, Celik E, Gonuldas F. Effect of different surface treatments on the biaxial flexural strength of zirconia ceramics. J Prosthet Dent. 2023;129:220e1-e5. https://doi.org/10.1016/j.prosdent.2022.11.008 ,

[15] Diken Türksayar AA, Demirel M, Donmez MB. Optical properties, biaxial flexural strength, and reliability of new-generation lithium disilicate glass-ceramics after thermal cycling. J Prosthodont: Online ahead of print. 2022. https://doi.org/10.1111/jopr.13632, PMID:36585789

[16] Huang CW, Hsueh CH. Piston-on-three-ball versus piston-on-ring in evaluating the biaxial strength of dental ceramics. Dent Mater. 2011;27:e117–23. https://doi.org/10.1016/j.dental.2011.02.011, PMID:21459428

[17] Isgrò G, Pallav P, van der Zel JM, Feilzer AJ. The influence of the veneering porcelain and different surface treatments on the biaxial flexural strength of a heat-pressed ceramic. J Prosthet Dent. 2003;90:465–73. https://doi.org/10.1016/j.prosdent.2003.08.003, PMID:14586311

[18] Thompson GA. Influence of relative layer height and testing method on the failure mode and origin in a bilayered dental ceramic composite. Dent Mater. 2000;16:235–43. https://doi.org/10.1016/S0109-5641(00)00005-1, PMID:10831777

[19] Wendler M, Belli R, Petschelt A, Mevec D, Harrer W, Lube T, *et al.* Chairside CAD/CAM materials. Part 2: flexural strength testing. Dent Mater. 2017;33:99–109. https://doi.org/10.1016/j.dental.2016.10.008, PMID:27884403

[20] Miranda JS, de Carvalho RLA, de Carvalho RF, Borges ALS, Bottino MA, Özcan M, *et al.* Effect of different loading pistons on stress distribution of a CAD/CAM silica-based ceramic: CAD-FEA modeling and fatigue survival analysis. J Mech Behav Biomed Mater. 2019;94:207–12. https://doi.org/10.1016/j.jmbbm.2019.03.011, PMID:30909025

[21] Homaei E, Farhangdoost K, Tsoi JKH, Matinlinna JP, Pow EHN. Static and fatigue mechanical behavior of three dental CAD/CAM ceramics. J Mech Behav Biomed Mater. 2016;59:304–13. https://doi.org/10.1016/j.jmbbm.2016.01.023, PMID:26896763

[22] Awada A, Nathanson D. Mechanical properties of resin-ceramic CAD/CAM restorative materials. J Prosthet Dent. 2015;114:587–93. https://doi.org/10.1016/j.prosdent.2015.04.016, PMID:26141648

[23] Albero A, Pascual A, Camps I, Grau-Benitez M. Comparative characterization of a novel cad-cam polymer-infiltrated-ceramic-network. J Clin Exp Dent. 2015;7:e495–500. https://doi.org/10.4317/jced.52521, PMID:26535096

[24] Lawson NC, Bansal R, Burgess JO. Wear, strength, modulus and hardness of CAD/CAM restorative materials. Dent Mater. 2016;32:e275–83. https://doi.org/10.1016/j.dental.2016.08.222, PMID:27639808

[25] De Jager N, de Kler M, van der Zel JM. The influence of different core material on the FEA-determined stress distribution in dental crowns. Dent Mater. 2006;22:234–42. https://doi.org/10.1016/j.dental.2005.04.034, PMID:16099031

[26] Tribst JPM, Dal Piva AMO, Madruga CFL, Valera MC, Borges ALS, Bresciani E, *et al.* Endocrown restorations: influence of dental remnant and restorative material on stress distribution. Dent Mater. 2018;34:1466–73. https://doi.org/10.1016/j.dental.2018.06.012, PMID:29935769

[27] Karaer O, Yamaguchi S, Nakase Y, Lee C, Imazato S. In silico non-linear dynamic analysis reflecting in vitro physical properties of CAD/CAM resin composite blocks. J Mech Behav Biomed Mater. 2020;104:103697. https://doi.org/10.1016/j.jmbbm.2020.103697, PMID:32174439

[28] Murakami N, Wakabayashi N. Finite element contact analysis as a critical technique in dental biomechanics: A review. J Prosthodont Res. 2014;58:92–101. https://doi.org/10.1016/j.jpor.2014.03.001, PMID:24709475

[29] Song JH, Wang H, Belytschko T. A comparative study on finite element methods for dynamic fracture. Comput Mech. 2008;42:239–50. https://doi.org/10.1007/s00466-007-0210-x

[30] Yamaguchi S, Mehdawi IM, Sakai T, Abe T, Inoue S, Imazato S. *In vitro in silico* investigation of failure criteria to predict flexural strength of composite resins. Dent Mater J. 2018;37:152–6. https://doi.org/10.4012/dmj.2017-084, PMID:28954942

[31] Greaves GN, Greer AL, Lakes RS, Rouxel T. Poisson's ratio and modern materials. Nat Mater. 2011;10:823–37. https://doi.org/10.1038/nmat3134, PMID:22020006

[32] Albakry M, Guazzato M, Swain MV. Biaxial flexural strength, elastic moduli, and x-ray diffraction characterization of three pressable all-ceramic materials. J Prosthet Dent. 2003;89:374–80. https://doi.org/10.1067/mpr.2003.42, PMID:12690350

[33] Vaidya A, Pathak K. Applications of Nanocomposite Materials in Dentistry. Woodhead Publishing; 2019, p. 285-305.

[34] Li QL, Jiang YY, Wei YR, Swain MV, Yao MF, Li DS, *et al.* The influence of yttria content on the microstructure, phase stability and mechanical properties of dental zirconia. Ceram Int. 2022;48:5361–8. https://doi.org/10.1016/j.ceramint.2021.11.079

[35] Yamaguchi S, Katsumoto Y, Hayashi K, Aoki M, Kunikata M, Nakase Y, *et al.* Fracture origin and crack propagation of CAD/CAM composite crowns by combining of in vitro and in silico approaches. J Mech Behav Biomed Mater. 2020;112:104083. https://doi.org/10.1016/j.jmbbm.2020.104083, PMID:32979609

[36] Skjold A, Schriwer C, Gjerdet NR, Øilo M. Fractographic analysis of 35 clinically fractured bi-layered and monolithic zirconia crowns. J Dent. 2022;125:104271. https://doi.org/10.1016/j.jdent.2022.104271, PMID:36041673

[37] Kirstein AF, Woolley RM. Symmetrical bending of thin circular elastic plates on equally spaced point supports. J Res Natl Bureau Standards, Sect C: Eng Instrum 1967:1.

[38] Choi SR, Bansal NP. Mechanical behavior of zirconia/alumina composites. Ceram Int. 2005;31:39–46. https://doi.org/10.1016/j.ceramint.2004.03.032

[39] Kelly JR, Benetti P. Ceramic materials in dentistry: historical evolution and current practice. Aust Dent J. 2011;56(suppl 1):84–96. https://doi.org/10.1111/j.1834-7819.2010.01299.x, PMID:21564119

[40] Giordano R, McLaren EA. Ceramics overview: classification by microstructure and processing methods. Compend Contin Educ Dent 2010;31:682–4, 6, 8 passim; quiz 98, 700.

[41] Li RWK, Chow TW, Matinlinna JP. Ceramic dental biomaterials and CAD/CAM technology: state of the art. J Prosthodont Res. 2014;58:208–16. https://doi.org/10.1016/j.jpor.2014.07.003, PMID:25172234

[42] Pereira GKR, Guilardi LF, Dapieve KS, Kleverlaan CJ, Rippe MP, Valandro LF. Mechanical reliability, fatigue strength and survival analysis of new polycrystalline translucent zirconia ceramics for monolithic restorations. J Mech Behav Biomed Mater. 2018;85:57–65. https://doi.org/10.1016/j.jmbbm.2018.05.029, PMID:29857261

[43] Kongkiatkamon S, Peampring C. Effect of speed sintering on low temperature degradation and biaxial flexural strength of 5Y-TZP zirconia. Molecules. 2022;27:5272. https://doi.org/10.3390/molecules27165272, PMID:36014509